Modeling and Simulation of Multi-Discipline Systems Using Bond Graphs and VHDL-AMS

F. Pecheux*, B. Allard†, C. Lallement‡, A. Vachoux§, H. Morel†
*LIP6/ASIM, Paris, France
†CEGELY, CNRS UMR 5005, INSA-Lyon, France
‡PHASE, Strasbourg, France
§EPFL, Lausanne, Switzerland

***Abstract*— Bond graphs represent a convenient tool for physical system analysis. While it is one part of the job to establish a pertinent bond graph model, it is another important part of the job to take advantage of this bond graph. A simulation tool is involved and the engineer effort varies depending on the sofware entry and computer issues. The paper focuses on the coherence of VHDL-AMS with regards to bond graphs. The objective is twofold. First the authors detail an experience on how to shift from a bond graph representation to a efficient VHDL-AMS code. Two practical examples are presented: a simple Pb-Fe battery and an airbag application. The essential of the language with respect to bond graphs is recalled. Second the authors discuss several advantages and limitations of the language with respect to other available languages and tools when it comes to modeling bond graphs. Then some possible evolutions for the next IEEE 1076.1 VHDL-AMS standard are outlined.**

I. KEYWORDS

VHDL-AMS, Electrochemistry, Battery cells, Chemical Reaction Kinetics, Airbag, Automotive engineering, Bond Graphs.

II. INTRODUCTION

Microelectronics and microtechnology combined several years ago to offer a major breakthrough: micro-opto-mechanical systems, or MOEMS. These systems are Systems-on-Chips, or SoCs. MOEMS combine multi-domain functions, tightly coupled to obtain successful products. Experts of various disciplines are required to work on the various functions. However, the final design is devoted to design engineers, most of them belonging to the electronic or technology community. Semiconductor companies report that SoCs or MOEMS are emerging slowly since the system-level optimization of the product remains empirical, thus unsatisfying. The main reason is the lack of system-level approach for the optimization. In fact microelectronics softwares are clearly separated into two categories: Electronic Design Automation (EDA) tools and technology softwares. The former addresses only mixed analog-digital circuits. The latter enables to manage the necessary steps to manufacture the device. There is still no available software on the market able to manage multi-discipline systems from both the microelectronics and microtechnology viewpoints.

When it comes to system-level modeling languages, the authors may conclude that the best candidate is the IEEE standard 1076.1 VHDL-AMS [Christen and Bakalar, 1999]. Verilog-AMS [Frey and O'Riordan, 2000] is not a IEEE standard yet. Both languages are largely used nowadays in chip design framework like Cadence [Cadence, 2004a]. However a language is only useful to represent equations and obtain simulation results. The system equations must be obtained through a multi-discipline analysis of the targeted system. Bond graphs are now established as quite universal technique to perform this analysis.

Lorenz [Lorenz, 1999] has proposed a classification of tools with respect to a modeling-level criterion. Bond graphs are classified in the "phenomenon modeling" area. Schematic diagram may only address the "component modeling" and it is the only available tool for a SoC design team at the moment. Lorenz classified also several languages like HDL-A, but it is limited to electrical and thermal domains. These latter limitations were considered as an input for the development of VHDL-AMS. Borutzky [Borutzky, 1999] was able to include VHDL-AMS into his comparison from object-oriented modeling point-of-view. VHDL-AMS is not so far an object-oriented language since inheritance has been proposed but not standardized yet [Benzakki and Djafri, 1997]. More recently, Borutzky [Borutzky, 2002] questionned the adequacy of VHDL-AMS to describe bond graphs. From a strict bond graph viewpoint, Borutzky is right, VHDL-AMS does not appear to be a suitable exchange format for bond graph models (unlike Modelica for example). One main reason for this statement is that VHDL-AMS uses the concept of generalized networks. Connection points are called ports, or *interface terminals*. The nature of the ports may be abstracted either as directional signal-flows, for both discrete-time and continuous-time models, or as satisfying conservative-law relationships between quantities, for continuous-time models only. Conservative-law relationships assume the existence of two classes of specialized quantities, namely *across* quantities that represent an effort (e.g., a voltage for electrical systems or a velocity for mechanical systems), and *through* quantities that represent a flow (e.g., a current for electrical systems or a force for mechanical systems). They also state that so-called General Kirchhoff Potential Law (GPL) and General Kirchhoff Flow Law (GFL) are met. These two laws are essentially the Kirchhoff's laws for electrical circuits generalized to any kind of conservative energy systems, e.g., mechanical, thermal, or fluidic systems. Together, across and through quantities form

a *nature*, that represents an energy domain, similarly to bond graphs. From an bond graph viewpoint, the consequence is that flow and effort variables have to be identified from two terminals as illustrated in Fig. 1. Signal flow description is

```
Entity capacitance is
        generic( c_value: real := 1u);
        port(terminal plus_armature, minus_armature: electrical);
end entity capacitance;
```

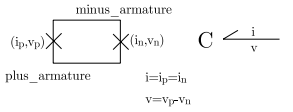

Fig. 1. Difference betweenVHDL-AMS terminals and bond graph ports

implemented in VHDL-AMS, but not in a power conservative manner as bond graphs may provide. The latter reasons explain why VHDL-AMS may not be an immediate exchange format for bond graphs. Unfortunately suitable tools like Modelica or Dymola are not used in Microelectronics community in contrary to VHDL-AMS.

The microelectronics and microtechnology community is looking for a common system-level description tool. System-level modeling yields equations, namely algebraic and differential equations, and these equations have to be implemented into a reference simulator, like Eldo [Mentor-Graphics, 2004], Smash [Dolphin-Integration, 2004], Spectre [Cadence, 2004b] or Spice [Berkeley-University, 2003], the most popular softwares in microelectronics. VHDL-AMS is the input language for many commercial products, that ensures compatibility with equivalent circuit models. The paper focuses on the coherence of VHDL-AMS with regards to bond graphs. The objective is twofold. The authors detail a shift from a bond graph representation to a VHDL-AMS code. Two practical examples are presented: a simple Pb-FE battery, and an air-bag application. Then the authors discuss several advantages and limitations of the language with respect to other available languages and tools. Then some specific limitations of VHDL-AMS are highlighted. Then some possible evolutions for the IEEE 1076.1 standard are outlined.

III. A SIMPLE Pb/Fe BATTERY MODEL

An extremely important class of oxidation and reduction chemical reactions is used to provide useful electrical energy in batteries. The authors detail a bond graph of a coupled system in which three forms of energy cohabit: chemical, thermal, and electrical. Second, the authors explain a solution to convert this bond graph model into its efficient VHDL-AMS equivalent source code.

Figure 2 presents a system schematic as a composition of an electrochemical Pb/Fe battery, an electrical resistor as a load, and a thermal network composed of thermal RC elements and an ambient temperature generator. When an electrical circuit is established between the cell and the resistor, the resistor heats and the resulting temperature modification is propagated to the RC thermal network. Temperature influences the thermodynamical conditions of the chemical reaction taking place inside the battery.

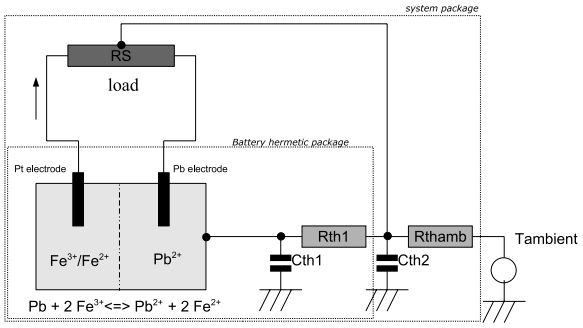

Fig. 2. The complete system, with chemical-electrical-thermal coupling.

Most of the chemical modeling presented in the paper relies on the methodological advices defined by Cellier [Cellier, 1991]. In particular, our battery model inherits from his work on gas reactions with suitable modifications.

A. Electrochemical issues

As shown in Figure 2, a complete $Pb/Pb^{2+}//Fe^{3+}/Fe^{2+}$ cell is built by associating one Pb/Pb^{2+} half-cell and one Fe^{3+}/Fe^{2+} half-cell. The electrode of the Fe^{3+}/Fe^{2+} half-cell is made of solid Platinum Pt (that does not participate in the chemical reaction) and the electrode of the Pb/Pb^{2+} half-cell is made of solid lead Pb. The corresponding half-reactions that take place inside the cell are given by equations (1) and (2).

$$Pb \rightleftharpoons Pb^{2+} + 2e^{-} \tag{1}$$

$$Fe^{2+} \rightleftharpoons Fe^{3+} + e^{-} \tag{2}$$

By running the half-reactions in separate containers, one can force the electrons to transit from the Pb/Pb^{2+} half-cell to the Fe^{3+}/Fe^{2+} half-cell through an external wire, which allows for the capture of as much as possible energy available as electrical work. When an electrical circuit is established between the two electrodes of the cell and the load resistor, Pb gets oxidized and Fe is reduced according to the complete following reaction (3)

$$Pb + 2Fe^{3+} \rightleftharpoons Pb^{2+} + 2Fe^{2+} \tag{3}$$

By convention, the electrical current goes from the Fe^{3+}/Fe^{2+} half-cell (place where Fe is reduced, i.e. the cathode) to the Pb/Pb^{2+} half-cell (place where Pb is oxidized, i.e. the anode).

The resulting cell ElectroMotive Force (EMF) u is given by equation (4)

$$u = E_{ox}(Pb) + E_{red}(Fe) = E_{ox}(Pb) - E_{ox}(Fe) \tag{4}$$

The larger the difference between the oxidizing and reducing forces of the reactants and products, the larger the cell

potential. The value of E_{ox} for a given susbtance is computed using the Nernst equation, that establishes the link between the number of moles of the ionic species involved and the resulting potential (5)

$$E_{ox} = E_{ox_0} - \frac{RT}{nF}\ln(\frac{a_{ox}}{a_{red}}) \quad (5)$$

where E_{ox_0} is the standard-state potential for a redox couple, R is the perfect gas constant, T the temperature, F the Faraday constant ($= 96500C.mol^{-1}$) and n the number of exchanged electrons . a_{ox} and a_{red} are called the activities of the ionic species involved in the half-reactions. These activities are proportional to the corresponding number of moles.

Applied to the Pb half-cell (1), equation (5) can be rewritten

$$E_{ox}(Pb) = 0.13 - \frac{RT}{2F}\ln(\frac{a_{Pb^{2+}}}{a_{Pb}=1}) \quad (6)$$

where 0.13 represents the standard-state potential of Pb/Pb^{2+} redox couple in Volts, $n = 2$ electrons are exchanged, and the activity of a_{Pb} is 1 by convention since it is a solid.

Accordingly, for the Fe_{3+}/Fe_{2+} half-cell, equation (5) becomes equation (7)

$$E_{ox}(Fe) = -0.77 - \frac{RT}{1F}\ln(\frac{a_{Fe^{3+}}}{a_{Fe^{2+}}}) \quad (7)$$

It is the resulting voltage u that is applied to the resistive source terminals. The rates at which, on one hand, Fe^{3+} decreases and, on the other hand, Fe^{2+} and Pb^{2+} increase is directly proportional to the current i flowing through the resistive source.

B. Bond graph modeling

Figure 3 details the bond graph that corresponds to the aforementioned system. The multiport elements involved are: the $0-$junctions, the $1-$junctions, the Capacitive Source CS, the Chemical Reactor ChR, the Thermal Capacitor Cth and Resistor Rth, the Ambient Temperature Generator ATG, and the Resistive Source RS.

Electrical and thermal bonds are well known, but chemical bonds require special attention. With regards to the power-oriented bond graph approach, the molar flow rate of a substance is naturally the appropriate flow variable for chemical. It is traditionally called ν or $\dot{n}$ in the litterature. Cellier [Cellier, 1991] states that "we must assume that an adjugate variable exists such that the product of the molar flow rate and its adjugate variable is chemical power. The adjugate variable has been coined the chemical potential of a substance, and its dimension is $J.mole^{-1}$. The chemical potential of a substance describes the amount of chemical energy stored in a mole of that substance". This adjugate variable is traditionally called μ, and corresponds to the effort variable requested by bond graphs. Shortly said, this means that a chemical substance x can store energy and thus can be represented by a capacitive source, like an electrical capacitor. The corresponding state variable for a chemical capacitor is n_x, the number of mole, and the state equation is $dn_x/dt = \dot{n_x} = \nu_x$. With reasonable

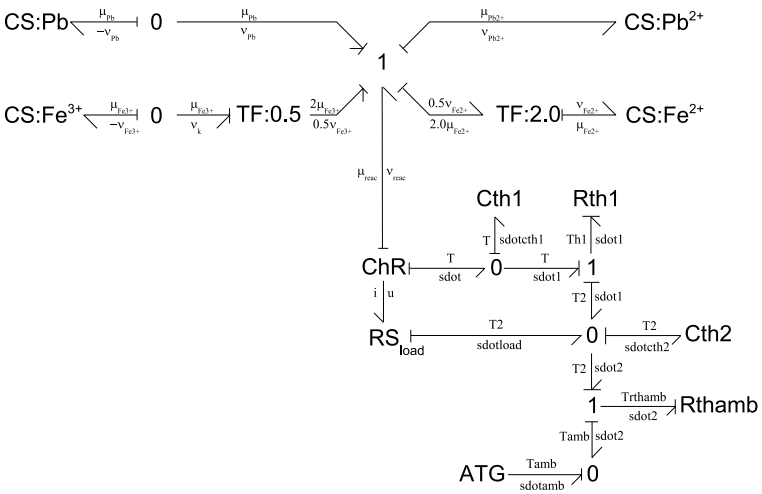

Fig. 3. A bond graph of the Pb/Fe battery system.

assumption, μ_x of the reactants in our battery can be considered as constant.

When the cell electrodes are both connected to the load resistor, an electrical circuit is established, and a current of electrons i flows through the resistor. The number of moles exchanged from the left side of equation (3) to the right side is conditioned by the presence of this current i as stated by the following equation

$$\nu_{reac} = \frac{i}{2F} \quad (8)$$

The chemical reaction is represented by a 5-port 1-junction. It receives chemical powers from the species Pb and Fe^{3+} and from the ChR element and delivers chemical powers to the species Pb^{2+} and Fe^{2+}. The bond graph clearly indicates that the ChR element is responsible for computing the voltage u. This voltage is used by the resistive source to calculate the current i, that gives in turn the molar flow of the equation ν_{reac}. At all times, the following equation concerning the molar flow for each species prevails

$$\nu_{reac} = \frac{i}{2F} = -\nu_{Pb} = -\frac{1}{2}.\nu_{Fe^{3+}} = \nu_{Pb^{2+}} = \frac{1}{2}.\nu_{Fe^{2+}} \quad (9)$$

To model the battery with greater accuracy, the voltage u is downgraded with thermal losses, expressed by equation (10)

$$u = E_{ox}(Pb) - E_{ox}(Fe) - \beta.\frac{\mu_{reac}.\nu_{reac}}{i} \quad (10)$$

Accordingly, the entropy flow generated by ChR is expressed by equation (11)

$$\dot{S} = \beta.\frac{\mu_{reac}.\nu_{reac}}{T} \quad (11)$$

From the thermodynamical viewpoint, current i generates an entropy flow in the electrical resistor that is propagated along the thermal network and reinjected in the ChR element as a temperature influence. The stoichiometric coefficients of reaction (3) are naturally represented by transformers.

C. VHDL-AMS implementation

Unlike bond graphs, VHDL-AMS distinguishes between the different kinds of power, and terminals are inherently strongly typed. Thus, a multi-domain bond graph yields to the writing of the corresponding domain-typed 0-junctions, 1-junctions and transformers. Figure 4 details the VHDL-AMS code for a 3-ports 1-junction in the electrical domain. Although it is quite easy to write and adapt to other domains, the code is not generic, and has to be rewritten for new port arities. For each port, the effort (resp. flow) variable of bond graphs becomes an $across$ (resp. $through$) $quantity$. The so-called *simultaneous statements* (lines 28 to 30) are direct transcriptions of the corresponding bond graph equations. Quantities correspond in VHDL-AMS to the unknowns of the system of equations to be solved by the analog solver. $Branch$ quantities are defined between two terminals (lines 24 to 26), and are opposed to $free$ quantities, i.e. quantities that are not $bound$ to any terminal. The generic clause (lines 11 to 13) allows for the redefinition of the three $sign$ variables with any value when the component is being instantiated.

```
1   library ieee;
2     use ieee.math_real.all;
3
4   library ieee_proposed;
5     use ieee_proposed.energy_systems.all;
6     use ieee_proposed.electrical_systems.all;
7
8   entity one3portsElectrical is
9     generic
10    (
11      sign1 : real := 1.0;
12      sign2 : real := 1.0;
13      sign3 : real := 1.0
14    );
15    port
16    (
17      terminal p1 : electrical;
18      terminal p2 : electrical;
19      terminal p3 : electrical
20    );
21  end entity one3portsElectrical;
22
23  architecture bhv of one3portsElectrical is
24    quantity mu1 across nu1 through p1;
25    quantity mu2 across nu2 through p2;
26    quantity mu3 across nu3 through p3;
27  begin
28    sign1 * mu1 + sign2 * mu2 + sign3 * mu3 == 0.0 ;
29    nu3 == nu1 ;
30    nu3 == nu2 ;
31  end architecture bhv;
32
```

Fig. 4. Listing for a 3-ports 0 junction, in VHDL-AMS.

The code for the Capacitive Source CS representing the species involved in the chemical reaction is given in Figure 5. For the moment, chemical systems are not directly supported in VHDL-AMS yet, and we have chosen to emulate the chemical domain by the electrical domain (lines 35 and 46). Because it is possible to name branch quantities by any identifier, this is not much of a problem (line 52). The $port$ clause (lines 46 to 47)is interesting, as it shows that both conservative c and signal-flow n terminals are used. As a part of the bond graph, the c terminal is conservative and obeys GKLs. The signal-flow quantity n corresponds to the number of mole of a substance and acts as a modulating signal that is propagated directly into the ChR element to compute the redox potentials. It is the reason why it has been declared in CS as a *out* signal-flow quantity. As in [Cellier, 1991], these modulating paths have been omitted from the bond graph. The if clause (line 54) searches for the quiescent point, and allows for the initialization of quantities and the handling of discontinuities. During initialization, the n quantities for all the species are not computed yet, and divisions by zero in the Nernst equation are therefore avoided. During transient analysis, the $else$ part of the if is executed, making the number of mole of the substance directly proportional to ν_{reac} (line 59). The $sign$ variable at line 59 is necessary because the simulator Advance-MS from Mentor Graphics does not manage flow directions properly when it computes the Jacobian matrix of the system. This is actually a problem because the chemical reaction goes from left to right, with a reaction constant of about 10^{30}. Other experiments have shown that in the case of reactions that go both ways, the $sign$ construct is unnecessary. The $'dot$ is an attribute that can be applied to any VHDL-AMS quantity. It is used to produce the signal-flow n, the number of mole of the substance.

```
33  library ieee_proposed;
34    use ieee_proposed.energy_systems.all;
35    use ieee_proposed.electrical_systems.all;
36
37  entity cs is
38    generic
39    (
40      mu0 : real := 1.0;
41      sign : real := 1.0;
42      nInit : real := 1.0
43    );
44    port
45    (
46      terminal c : electrical;
47      quantity n : out real
48    );
49  end entity cs;
50
51  architecture bhv of cs is
52    quantity mu across ndot through c;
53  begin
54    if domain=quiescent_domain use
55      mu == mu0 ;
56      n == nInit;
57    else
58      mu == mu0 ;
59      n'dot == sign * ndot;
60    end use;
61  end architecture bhv;
62
```

Fig. 5. Listing for the chemical Capacitive Source CS, in VHDL-AMS.

The complete code for the Pb/Fe battery cell can be found at ([Pecheux et al., 2004a]).

Figure 6 exhibits some simulation results. The initial number of moles for species Fe^{3+}, Fe^{2+} and Pb^{2+} are respectively $0.05, 0.01$ and 0.1 in our example. When the battery has been completely discharged, Fe^{3+} is zero, $Fe^{2+} = 0.01 + 0.05 = 0.06$ moles, and $Pb^{2+} = 0.1 + 0.025 = 0.125$ moles, as shown on the Figure 6. The number of moles of electrons flowing through the resistor is exactly 0.05, (cf. equation 2). The battery can therefore produce $0.05 * 96500 = 4825C = 1.34A.h$. For a RS value of 0.012Ω, the battery is discharged in approximatively 1 minute, but the current is about $80A$. One can notice that the voltage u of the battery is zero when $E_{ox}(Pb) = E_{ox}(Fe) = 0.157V$. To obtain exactly this value for $E_{ox}(Fe)$, the corresponding number of moles is $1.2516e^{-17}$!!! We are currently investigating the effect of temperature on the battery behavior.

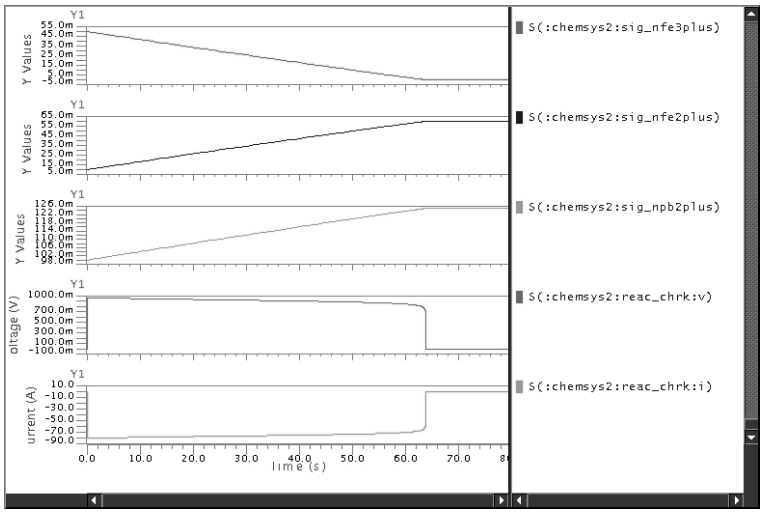

Fig. 6. Simulation of the Pb/FeBattery.

IV. An airbag example

The same methodology has been applied to an airbag, a succesfull mechatronic product [Pecheux et al., 2005]. Current developments are targeting a monolithic implementation. It is then a significant example to discuss the combination of bond graphs and VHDL-AMS. Basically a SoC airbag is made of 2 parts. One visible part is the cushion (Fig. 7). The other part is hidden, and contains the sensor, the actuator and the control system.

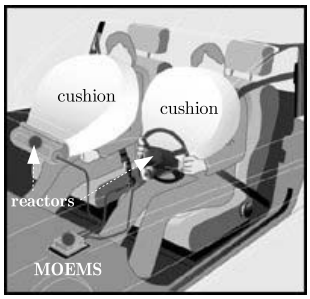

Fig. 7. Typical SoC airbag system inside a car

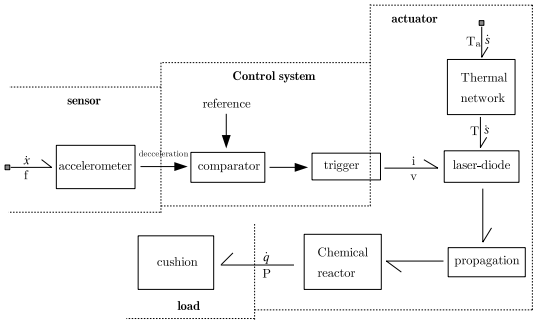

Fig. 8. Schematic of a SoC airbag.

A. System-level model

The control system (Fig. 8) is essentially digital and computes a so-called *crash-algorithm*. The control system takes a decceleration value as an input data from the sensor (accelerometer). Bond graphs do not offer a better modeling than a signal flow description. From a technological point of view, this part is based on a processor and digital hardware. The essential remains the algorithm. In fact, bond graphs help in the analysis of pure analog functions: the accelerometer, the trigger output stage, the laser-diode, the propagation link and the chemical reactor. The accelerometer is a pendulum or a tethered seismic mass. The mass displacement is transformed into variations of charge and capacitive effects. The control system turns-on the CMOS output stage of the trigger. The power stage produces the laser-diode illumination, and optical power is propagated through a dedicated link to the chemical reactor. The actuator is in fact a generator of inert gaz (N_2) that inflates the cushion.

For the sake of place, the authors do not detail the airbag but VHDL-AMS source code are available on a dedicated website [Pecheux et al., 2004b]. Litterature reports the example of a mass coupled to piezoelectric phenomenon [Granda, 2002]. Piezoelectric phenomenon has been modeled as a transformer in a first approach. A suitable sensor conditioner extracts the generated charges and produces a capacitive output impedance. This impedance is related to the mass behavior. The control system is modeled as a signal flow-graph, except the CMOS power output stage related to semiconductor devices. An already published approach is considered [Morel et al., 1995] [Lallement et al., 1997] [Allard et al., 1997]. The laser-diode is a photo-diode represented by a switched bond graph. A leakage current models the diode when not illuminated. A non-linear current source models the illumination current. Both currents are injected into a resistor/capacitor network. The non-linear current source depends on the device temperature, mainly influenced by the ambiant temperature. A transformer links the electrical and optical domain. A pseudo bond graph is used. The optical link between the laser-diode and the chemical reactor is modeled in terms of propagation effects as in [Morel et al., 2003].

B. The chemical reaction

The cushion is folded so that to inflate as fast as possible. A solid propergol capsule (NaN_3) is used with a special coating to keep it inert. Optical power is enough to degrade severely the coating and to enable the explosive reaction. The same effect may be obtained using a spark. All species are solid but azote. An oxydo-reduction reaction takes place and produces azote and sodium. NaN_3 is a powerful reductor due to a ionic composition. The ionic system is characterized by a delocalized electron cloud, stimulated by light. KNO_3 and SiO_2 are oxydant species. Unfortunately solid sodium is poisonous, and the two latter reactions of (15) are necessary to convert Na into an inert species. $K_2Na_2SiO_4$ is a kind of glass.

$$2NaN_3 \rightarrow 2Na + 3N_2 \quad (12)$$

$$10Na + 2KNO_3 \rightarrow K_2O + 5Na_2O + N_2 \quad (13)$$

$$K_2O + Na_2O + SiO_2 \rightarrow K_2Na_2SiO_4 \quad (14)$$

First,a computation has been performed to yield the enthalpies, entropies and free Gibbs energy of formation for the individual species, using the following relations where C_p is a specific heat ($J.K^{-1}.mol^{-1}$). The standard molar enthalpy of formation, $\Delta_f H_{298}$ and the reference entropy, S^0_{298}, are tabulated in litterature for each individual species.

$$\begin{aligned} \Delta H_T &= \Delta_f H_{298} + \int_{298}^{T} C_p dT \\ S^0_T &= S^0_{298} + \int_{298}^{T} \frac{C_p}{T} dT \\ \Delta G &= \Delta H + T.\Delta S \end{aligned} \quad (15)$$

It is then possible to appreciate the virulence of each reaction for various temperature. At room temperature, the first reaction of (15) is characterized by $\Delta G = -1424 kJ.mol^{-1}$. This tremendous value explains the explosive behavior of the reaction. Both reactions take place at room temperature since entropy excess of reaction (12) is consumed partialy by the other reactions. Isothermic conditions are considered. Pressure does not influence significantly reactions of solid species. Thermodynamic computations show that the chemical process only evolves as indicated in the first reaction of (12). Probably from system-level point of view, it is sufficient to model only this first reaction as it produces 90% of the required inert gaz. Equations 15 do not give access to the chemical dynamics.

As said previously, the authors have found two approaches as reported in [Cellier, 1991] and [Thoma and Bouamama, 2000] respectively to build a bond graph, i.e. a state-variable model. The state-variables are of 6 types, namely, T, S, p, V, μ_i (chemical potential) and $\dot{n}_i$ (molar flow rate). Authors have followed the ideas developed by Cellier when inert gaz is involved (reactions (1) and (2)), and Thoma's approach for solid species reaction (reaction 3 of (15)). However if reaction (1) is taken alone, similar results are obtained using the method developped by Thoma, though authors are not able to discuss the necessity of entropy stripping and unstripping. It is assumed that the molecules are mixed in a completely homogeneous manner. Of course the assumption may not be experimentaly verified, but remains a fair assumption in the case of very fast reactions.

Similarly to the battery example, equations give the molar flow of each equations. The ideal gas equation is used for the inert gaz as a state equation. The Gibbs and Gibbs-Duheim equations are used as other state equations. The Gibbs relation yields the entropy flow associated with a given reaction, and the Gibbs-Duheim relation yields the term $\dot{\nu}_i$. A capacitive source is associated to each species, and accumulates mass. Each $\dot{n}_k$ relation is associated to a 0-junction. A chemical reactor element, ChR, is associated to a 1-junction related to the related species of the reaction. ChR balances the chemical powers into or out of the reaction with thermic and hydraulic powers. It looks like an RS component. Finaly a bond graph has been established, and the system equations have been coded using VHDL-AMS. Figure 9 pictures simulation results. Fig. 9 shows the evolution of various species and particularly N_2. The inert gas is generated whithin 20ms, i.e. a number comparable with experimental data. A zoom on the evolution of Na shows that the 2 reactions involved in the neutralization of the Na, are quite slow compared to the explosive first reaction. For sure, A EDA engineer may not interact with the chemical part, but he may check the influence of semiconductor-level optimization at system-level, using the EDA tools like VHDL-AMS.

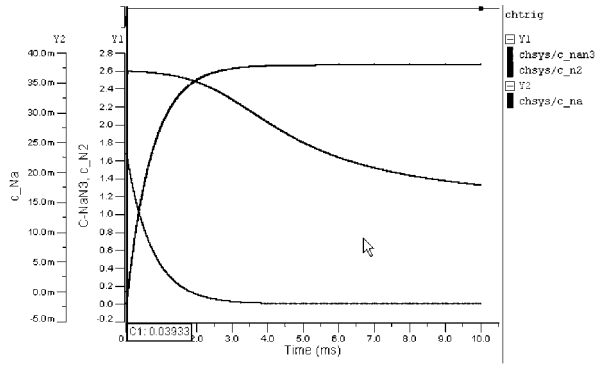

Fig. 9. Simulation of azote generation

The airbag main specifications are: sensitivity, reliability and efficiency. Sensitivity is related to the accelerometer, the ability of the control system to deal with the sensor non-linearity and the propagation link performances. Reliability is related to the crash-algorithm but also to the thermal behavior of the laser-diode. Efficiency is mostly related to the critical path from the sensor input to the cushion, and involves the digital hardware as well as the laser-diode rise-time and the chemical reaction velocity. As a conclusion, all functions inside the airbag are coupled.

V. Discussion

On one side, it is the EDA engineer that is the final designer of the monolithic system. Because of his curriculum, he is unable to estimate the impact of an integration effect on the

system performances, except if he relies on a system-level model. On the other side, only discipline experts are able to specify each part of the system. A bond graph offers a common representation, and VHDL-AMS can be the common tool for the EDA engineers. The commented VHDL-AMS codes show that 2 terminals are necessary to represent one bond graph port, as reported previously by Borutzky [Borutzky, 1999]. The authors do not pretend that VHDL-AMS is an exchange format for bond graphs. First VHDL-AMS is necessary in the microelectronics community, and the 2-terminals remark is true, obviously it is unelegant and heavy, but the above examples demonstrate that simulation is successful. VHDL-AMS also proposes a *procedural statement*. Unlike the previous simultaneous statement, a procedural statement allows for the execution of a piece of sequential (ordered) list of statements (equations). Namely it would enable to take advantage of the causality analysis. Unfortunately current releases of Advance-MS do not support this important feature.

Genericity and object-oriented modeling are not supported yet by VHDL-AMS. For example, a junction model has to be repeated for each energy domain. It does not limit the language simulation capabilities but introduces unnecessary development.

Authors are preparing two contributions to be submitted to the IEEE 1076.1 VHDL-AMS working group. Several energy domain descriptions are missing. Obviously a *chemical_domain* standard should be added. The *across* quantity is the chemical potential (μ in J.mol^{-1}) and the *through* quantity is the molar flow ($\dot{n}$ in mol.s^{-1}). An other contribution addresses the object-oriented modeling capabilities.

VHDL-AMS, like Modelica and Dymola, suffers from the lack of homogeneity control. The VHDL-AMS compiler parser does not actually perform semantic checks on the homogeneity of equations. Obviously, this feature would prevent quite a lot of errors. The university package, Pacte [Morel et al., 1990], and the associated HDL language, M++, provide this feature.
This package also enables to debug step-by-step the system equations. This feature is related to the computer tool that implements the language. Quite all commercialy available software miss satisfying debug capabilities.

VI. Conclusion

Authors have reported an experience of multi-discipline system modeling using bond graphs and simulation using VHDL-AMS. The latter example, the airbag, is sufficiently large to demonstrate VHDL-AMS simulation capabilities. Some limitations exist in the language that do not affect the simulation capabilities but make the development more tedious. Contributions will be proposed to the IEEE 1076.1 VHDL-AMS working group to solve some limitations inherent to bond graphs such as the description of energy domains other than electricity and thermics. Object-oriented modeling would be also a significant improvement.

Microelectronics and microtechnology community is actually held by major players in the EDA and process software like Cadence, Mentor Graphics, Synopsys or Silvaco. It is unthinkable to change the profession milestones by now, but it is the time for linking these domains and tools together, by developing the appropriate economic bonds [Thoma and Bouamama, 2000], on page 167. VHDL-AMS could be one of the variables...

References

[Allard et al., 1997] Allard, B., Morel, H., Ammous, A., and Ghedira, S. (1997). Extension of causality analysis to bond graphs including state–space models. *Proc. of ICBGM*, 29(1):72–78.

[Benzakki and Djafri, 1997] Benzakki, J. and Djafri, B. (1997). Object-oriented extensions to VHDL- the lami proposal. *Proc. of CHDL*, pages 334–347.

[Berkeley-University, 2003] Berkeley-University (2003). Spice 3f5. Technical report. www.repairfaq.org/ELE.

[Borutzky, 1999] Borutzky, W. (1999). Bond graph modeling from an object oriented modeling point of view. *Elsevier, Simulation Practice and Theory*, 7(5/6):439–461.

[Borutzky, 2002] Borutzky, W. (2002). Bond graphs and object oriented modeling - a comparison. *Systems and Control Engineering, part-I*, 216(11):21–33.

[Cadence, 2004a] Cadence (2004a). framework overview. Technical report. www.cadence.com.

[Cadence, 2004b] Cadence (2004b). Virtuoso SPECTRE circuit simulator. Technical report. www.cadence.com/products/custom_ic/spectre.

[Cellier, 1991] Cellier, F. (1991). *Continuous system modeling*. Springer, Berlin, Germany.

[Christen and Bakalar, 1999] Christen, E. and Bakalar, K. (1999). VHDL-AMS a hardware description language for analog and mixed signal applications. *IEEE Trans. on Circuits and Systems, part -II*, 46(10):1263–1272.

[Dolphin-Integration, 2004] Dolphin-Integration (2004). Smash 5.3: logic, analog and mixed simulation. Technical report. www.dolphin.fr/medal/smash.

[Frey and O'Riordan, 2000] Frey, P. and O'Riordan, D. (2000). VERILOG-AMS mixed-signal simulation and cross domain connect modules. *Proc. of IEEE/ACM International Workshop on Behavioral Modeling and Simulation*, pages 103–108.

[Granda, 2002] Granda, J. (2002). The role of bond graph modeling and simulation in mechatronics systems. an integrated software tool: CAMP-G, MATLAB-SIMULINK. *Mechatronics*, (12):1271–1295.

[Lallement et al., 1997] Lallement, C., Bouchakour, R., and Maurel, T. (1997). One-dimensional analytical modeling of the VDMOS transistor taking into account the thermoelectrical interactions. *IEEE Trans. on Circuits and Systems, part-I*, 44(2):103–111.

[Lorenz, 1999] Lorenz, F. (1999). A classification of modeling languages for differential-algebraic equations. *Elsevier, Simulation Practice and Theory*, 7(5/6):553–562.

[Mentor-Graphics, 2004] Mentor-Graphics (2004). Analog-mixed signal ELDO RF. Technical report. www.mentor.com.

[Morel et al., 2003] Morel, H., Allard, B., Ammous, K., Garab, H., Bergogne, D., and Auriol, P. (2003). Transmission line and bond graphs. *Proc. of ICBGM*, 35(1):148–156.

[Morel et al., 1990] Morel, H., Allard, B., and Chante, J. (1990). Pacte: a behavioral simulator for power electronics. *Proceedings of IMACS–TC1*, 2:411–416.

[Morel et al., 1995] Morel, H., Allard, B., Lin, C., and Helali, H. (1995). Semiconductor device modeling and simulation using bond graphs. *Proc. of ICBGM*, 27(1):269–274.

[Pecheux et al., 2004a] Pecheux, F., Allard, B., Lallement, C., Vachoux, A., and Morel, H. (2004a). Vhdl-ams source code of a pb/fe battery, and chemical aspects in an airbag model. Technical report. http://lsmwww.epfl.ch/icbgm05.

[Pecheux et al., 2004b] Pecheux, F., Lallement, C., and Vachoux, A. (2004b). Vhdl-ams/verilog-ams source codes of an airbag model. Technical report. http://lsmwww.epfl.ch/tcad.

[Pecheux et al., 2005] Pecheux, F., Lallement, C., and Vachoux, A. (to be published in 2005). Vhdl-ams and verilog-ams as alternative hardware description languages for efficient modeling of multi-discipline systems. *IEEE trans. on Computer Aided Design*.

[Thoma and Bouamama, 2000] Thoma, J. and Bouamama, B. O. (2000). *Modelling and simulation in thermal and chemical engineering*. Springer, Berlin, Germany.